A novel method for remediation of nickel containing wastewater at neutral conditions

Haruko Hase[a], Toru Nishiuchi[a] Tsutomu Sato[b,] *, Tsubasa Otake[b], Tsuyoshi Yaita[c], Tohru Kobayashi[c], and Tetsuro Yoneda[b]

[a] Graduate school of engineering, Hokkaido University, Kita 13 Nishi 8, Kita-ku, Sapporo, 060-8628, Japan

[b] Faculty of engineering, Hokkaido University, Kita 13 Nishi 8, Kita-ku, Sapporo, 060-8628, Japan

[c] Materials Sciences Research Center, Japan Atomic Energy Agency, 1-1-1 Koto, Sayo-cho, Sayo-gun, Hyogo, 679-5148, Japan

*Corresponding author: Tel: +81 11 706 6305, e-mail: tomsato@eng.hokudai.ac.jp

Graphical abstract

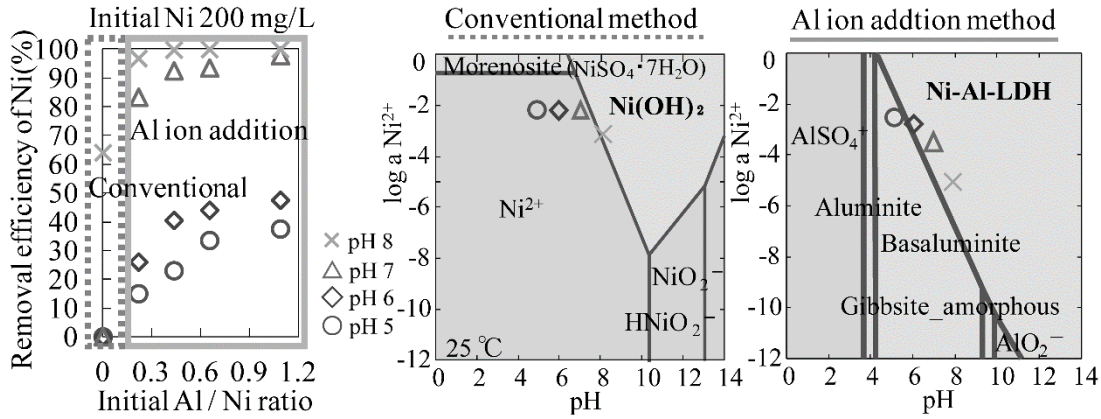

Highlights

- High Ni removal efficiencies at neutral pH conditions were achieved.
- Layered double hydroxide was selectively precipitated by the addition of Al ions.
- Ni was mainly incorporated into the hydroxide structure at pH 7 and 8.
- A thermodynamic geochemical model reproduced the experimental results well.
- Ni can be removed by adding a small amount of Al ions in practical wastewater treatment.

Keywords

Layered double hydroxide; Nickel; Aluminum; Wastewater treatment; Geochemical modeling

Abstract

Heavy metals contained in wastewater are generally removed by adding antalkaline to increase the pH, and Ni is commonly precipitated as Ni-hydroxides at pH 10. However, a more sustainable

remediation method of treatment at neutral conditions would be attractive due to the high cost of chemical reagents and inefficient treatment at present. Based on natural attenuation, the method of adding Al ions has been used in wastewater treatment to precipitate layered double hydroxides (LDH). Here, we investigated the use of Al ion addition in the Ni containing wastewater treatment, experimentally and thermodynamically. By co-precipitation experiments adding Al ions to Ni-containing water, Ni was selectively incorporated into the structure of LDH, and the removal efficiency of Ni was close to 100% even in pH 7 and 8 samples (lower pH than conventional methods) with initial Ni concentrations of 200–10,000 mg/L. Geochemical modeling results replicate the experimental results well when the Al/Ni ratio of LDH is assumed to be0.33. This model makes it possible to estimate the amount of Al ions and additive agents necessary for use in treatment of wastewater containing different Ni concentrations.

1. Introduction

Advances in technology such as the electronics and metal plating industries have increased the demand for Ni [1], and some industrial wastewaters contain large amounts of Ni, leading to environmental pollution as excessive intake of heavy metals is harmful to humans and as wastewaters lead to environmental pollution. Hence, there is a need to maintain the environmental standards for Ni and to dispose properly of stable precipitation products to protect human health and protect natural environments. At the same time, Ni-rich mines and grades of Ni ore have been decreasing with the increase in mined quantities of Ni [2]. Additionally, resources are unevenly distributed and found only in a few countries making the supply sources of Ni vulnerable. Because of this, there is an urgent need to recover Ni from wastewaters and other waste forms.

Current wastewater treatments can be divided into biological [3–8] and chemical treatment methods [9–15]. Chemical precipitation processes (especially hydroxide precipitation) are widely used among these treatments [16,17]. Generally, the removal of Ni from wastewater by adding antalkaline and flocculants to increase the pH to 10 (the lowest solubility of Ni) or above result in the generation of Ni-hydroxides, and after treatment it is necessary to decrease the pH below the effluent standards of Japan (pH5.8–8.6) before discharge. However, the current method suffers from disadvantages including the high cost of antalkaline, flocculant reagents, and acid neutralizing agents. Therefore, it would be useful to develop a lower-cost and still effective wastewater treatment. The concentration of heavy metals and toxic ions in soils and ground waters may be attenuated in natural processes such as neutralization and mineral precipitation [18,19]. The natural attenuation processes may be applied to wastewater treatment, something which would likely be safer, more environmentally friendly, and more cost-effective, than conventional methods. For example, a study [20] has clarified the natural attenuation mechanism of Cu and Zn ions at Dougamaru, an abandoned mine in Japan. The mine drainage here contains higher concentrations of Cu and Zn ions than effluent regulatory

limits in Japan allow (3 mg/L for Cu and 2 mg/L for Zn). However, Cu and Zn in the mine drainage are incorporated in the structure of precipitates composed of Cu-bearing layered double hydroxides, hydrowoodwardite at around pH 6 because this is produced by the presence of Al ions in the drainage, resulting in natural attenuation. The general chemical composition formula of layered double hydroxide (LDH) is represented by $[M^{2+}_{1-x}M^{3+}_{x}(OH)_2(A^{n-})_{x/n}\cdot mH_2O]$ ($0.20 < x < 0.33$), and LDH is classified as anionic clay because of its anion exchange capacity [21,22]. It has a structure of octahedral hydroxide layers with alternating laminated interlayers of anions (A^{n-}) and inter-layer water. In LDH, substitution of the divalent cation (M^{2+}) with a trivalent cation (M^{3+}) produces a positive charge on the hydroxide layers, requiring the presence of anions between the hydroxide layers to maintain the charge balance. Nickel could be incorporated in the LDH octahedral sheets because hydroxide layers of LDH are essentially composed of metal ions with coordination number 6.To further explore this, the objective of this study is to investigate the optimum conditions such as pH, Al, and Ni concentrations under which Ni-LDH is precipitated by the addition of Al ions and compare this with the conventional method to precipitate $Ni(OH)_2$, to under-stand the behavior of Ni in the precipitation process, and to develop a geochemical model to reproduce the experimental results. With these results, the final goal is to develop a remediation method for Ni-bearing wastewaters at neutral conditions and to investigate the applicability of the Al ion addition method for Ni-containing water using the model.

2. Experimental

Co-precipitation experiments were carried out to synthesize Ni-bearing LDHs with different Al/Ni ratios to confirm the applicability of LDH in Ni-bearing wastewater treatment. However, the uptake mechanism of Ni is considered to be complex because multiple slightly soluble salts are simultaneously precipitated in the co-precipitation processes. Therefore, adsorption experiments were also carried out to elucidate the adsorption behavior of Ni onto the precipitated phases. In addition, extraction experiments were carried out to establish details of the chemical state of Ni in the precipitated phases.

2.1. Co-precipitation experiments

Co-precipitation experiments were carried out in Ni-containing water with SO42−by Al ion addition under various conditions (pH, Al, and Ni concentrations) to establish whether Ni-LDH is precipitated and what the precipitating conditions of Ni-LDH are. Initially, simulated wastewaters were obtained by mixing NiSO4·6H2Oand Al2(SO4)3·14–18H2O (Kanto Chemical Co., Inc.,

Guaranteed reagent) with 150 mL deionized water in 250 mL polyethylene bottles, then alkaline titrated by adding 1.0 M NaOH was below1 mL/min at 25◦C, and adjusted to set pH values with vigorous stir-ring (300 rpm). The initial Ni concentrations were set to 200, 1000, and 10,000 mg/L because the actual wastewater contains various Ni concentrations, and the resulting initial Al/Ni molar ratios were0, 0.218, 0.435, 0.653, and 1.087 to for determining the influence of the amount of Al ions. The resulting molar ratio is complicated by the fact that the unit of the initial concentration was set to "mg/L" as widely used in wastewater treatment (f.ex., the initial Al/Ni molar ratios of the solution with initial Ni and Al ion concentrations were respectively 1000 mg/L and 200 mg/L is 0.218). The pH values were5.0, 6.0, 7.0, and 8.0 (±0.1) allowing confirmation of the precipitates at neutral conditions. After titration, the suspensions were left standing for 24 h at 25◦C. The supernatant solutions were collected by centrifugation for 40 min at 3000 rpm, and the solid phases were recovered after solid-liquid separation. The extraction experiment is a quantitative evaluation achieved by dissolving or extracting only specific components of the solid or liquid using different types of solvents. The first step was deionized water (pH 5.8) extraction for water soluble ions from the solid phases and the second was CaCl2extraction for the exchangeable ions around pH 6.5, using CaCl2solutions of 3.0, 15, and 150 mmol/L (in solutions respectively with 200, 1000, and 10,000 mg/L of initial Ni) [23,24]. The maximum concentration where Ni was adsorbed was considered the Ca concentration. The solid and suspension were shaking for 24 h at 200 rpm at 25◦C and the liquid-solid ratio was 500 mL/g, and then were separated. Adsorption experiments were also carried out to determine the Ni adsorption behavior of each of main precipitates generated by the co-precipitation experiments. The adsorption solutions were30 mL with Ni concentrations of 10, 50, 100, 300, and 1000 mg/L using Ni(NO3)2·6H2O suspended in 0.02 M NaNO3as a supporting electrolyte solution at pH 5.45–5.60. Next, 100 mg of the solid phases were added to the solutions (giving a liquid-solid ratio of300 mL/g). The solid and liquid phases were separated for the further analysis after shaking for 24 h at 25℃.

2.2. Analytical methods

The concentrations of Ni and Al ions contained in the recovered solutions after the treatments were analyzed by inductively coupled plasma atomic emission spectrometry (ICPE-9000, Shimadzu). The SO42−ions contained in the supernatant were quantitatively analyzed by using ion chromatography (Metrohm 861 Advanced Compact IC). Compact IC is comprised of 3 consecutive suppressor units that are used for suppression, regeneration with sulfuric acid (0.04 M), and rinsing with ultrapure water. The eluent was diluted mixed solution of Na2CO3(2.70 mM) and NaHCO3(0.30 mM). The column was set to 35–38℃.The solid phases were freeze dried and were then analyzed to determine

the mineral component of the precipitates. The minerals contained in the solid phases were analyzed by X-ray diffraction. The precipitates were examined using an X-ray diffractometer (Multi Flex, Rigaku, Japan) equipped for graphite-monochromatic CuKα radiation at 40 kV and 40 mA. The randomly oriented powder samples were scanned at 2θ from 5°to 70°at the scanning speed of 3.0° (deg 2 θ/s).The X-ray absorption fine structure (XAFS) spectra of the Ni K-edge were measured to determine the chemical states of Ni in the precipitates. Co-precipitation samples and standard samples of Ni(OH)2(Wako Pure Chemical Industries, Ltd., Guaranteed reagent), NiO, NiSO4·6H2O (Kanto Chemical Co., Inc., Guaran-teed reagent), and synthesized takovite (Ni6Al2(OH)16CO3•5H2O) [25–28] where the structure and composition are known were measured under the same conditions. The XAFS spectra of the Ni K-edge was obtained by transmission XAFS measurement at BL-7C using an Si (111) two-crystal monochromator and scanned from7826.7 eV to 9431.5 eV. The X-ray absorption at the Near Edge Structure (XANES) was analyzed using REX software to compare the spectrum of the standard and co-precipitated samples qualitatively. In addition, the Extended X-ray Absorption Fine Structure(EXAFS) was analyzed using WinXAS 3.2 to clarify the local structure around the Ni contained in the samples. The zeta potential of the precipitates was measured in a solution using a Zetasizer nano series Nano-ZS90, Malvern. Samples with the liquid-solid ratio 10,000 mL/g using deionized water were adjusted to pH 4–12 by acid and alkaline titration using 0.10 M HNO3as the acid solution and 0.10 M NaOH as the alkaline solution.

3. Results and discussion

3.1. Characterization of the liquids and solids after co-precipitation

3.1.1. Liquid

The efficiency of removal of Ni from the synthetic wastewater is shown in Fig.1. Conventionally, without Al addition at pH 7 or lower, the Ni removal efficiency is very nearly 0% and no solid phases were observed. With increasing initial Al/Ni ratios, the efficiency increased to more than 16% at pH 5 and to almost 100% at pH 7 and 8. In addition, the efficiency was high with high initial Al/Ni molar ratios and high pH. With increasing initial Ni concentration, the removed percentage of Ni was rising steadily. In this study, the target Ni concentration after the water treatment was set at 1.0 mg/L (the permissible exposure limit of soluble nickel for worker health, as regulated by the Occupational Safety and Health Act), this set value is the highest limit of major standards reported by organizations of other countries. In some experiments at pH 8, a dissolved Ni concentration

below 1.0 mg/L was achieved. The concentration of Al ions was below the detection limit, and the removal efficiency of SO_4^{2-} showed changes similar to those of Ni (data not shown).

3.1.2. Solids

Figure 2 shows XRD patterns of co-precipitation products at different pH values. Broad peaks of Ni-Al-LDH are observed in all samples with the addition of Al ions, and the diffraction patterns appear similar to those shown in a previous study [29]. Peak positions around 10 and 20° in the 2θ of basaluminite [Al_4 (SO_4) (OH) $_{10}$•5(H_2O)] [30] are at lower angles than those of LDH. In addition, the peak intensity around 20° in 2θ is higher than that around 10° in 2θ in basaluminite, opposite that in LDH. At low pH (especially pH 5), the peak around 20° in 2θ has become prominent as in basaluminite. In addition, the peak positions around 10 and 20° in 2θ shifted to the lower angle side relative to those of LDH and were closer to those of basaluminite. This result suggests that low crystallinity basaluminite was precipitated, peaks of highly crystalline aluminite [Al_2 (SO_4) (OH) $_4$•7(H_2O)] were observed at pH 5 and 6. From these results, it may be concluded that basaluminite and aluminite were dominantly precipitated with small amounts of LDH at pH 5. Then, with increasing pH, the precipitated amounts of LDH increased and those of Al minerals decreased, and at pH 7 and 8 LDH was mainly precipitated. The XRD patterns in this precipitate were similar to those in samples with different initial concentrations or initial Al/Ni molar ratios.

The Ni K-edge XANES spectra and the radial distribution function profiles (RDF profile) of the standards and the precipitates at different pH are shown in Fig. 3(A) and (B), respectively. From the XANES spectra, the normalized height of the pre-edge peak at the low energy side of the X-ray absorption edge (around 8330 eV) was about 0.01 in all samples. A previous study [31] explained that the pre-edge height of Ni with 6-fold coordination (around 0.020) is twice or three times that of Ni with 5 or 4-fold coordination (0.036 and 0.062), that is, the pre-edge height increases when the coordination number increases from 4 to 6. This suggests that the coordination number of Ni in the precipitates was 6. From the RDF profile, the precipitates were very different from the NiO structure. It would appear that at pH 7 and 8, Ni ions were incorporated into LDH octahedral sheets because the profiles of the precipitates were similar to those of takovite and $Ni(OH)_2$. The second coordination shell(Ni-Ni) of precipitates as well as $NiSO_4 \cdot 6H_2O$ become less prominent at pH 5 and 6 than at 7 and 8. Possible reasons for this would be that the precipitated amount of Ni minerals was small and Ni ions were taken up as in basaluminite (whose structure is similar to that of LDH).

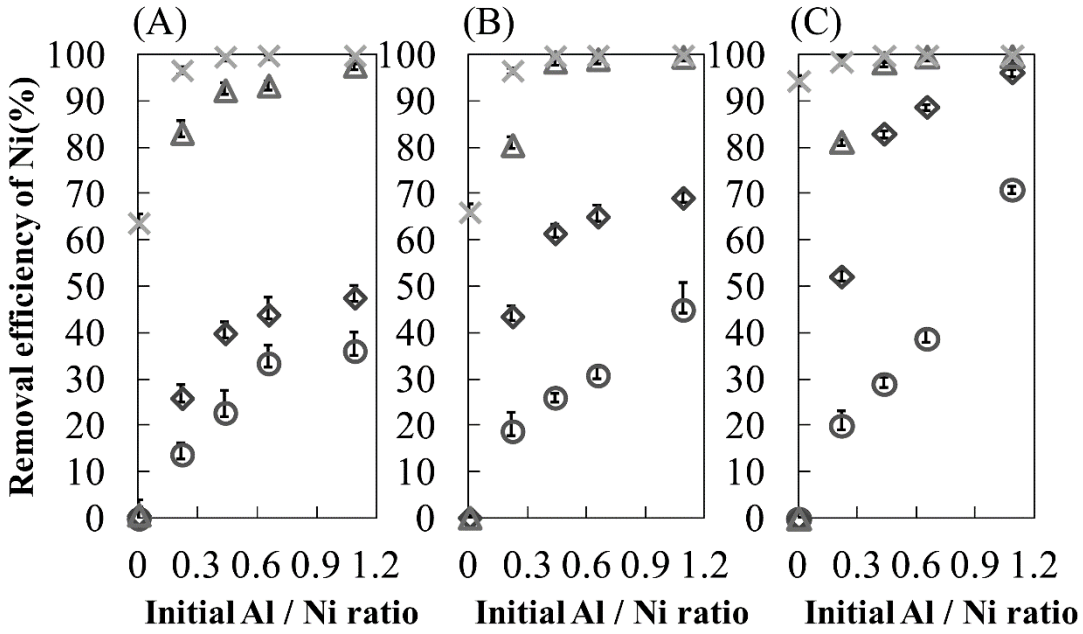

Fig. 1. Removal efficiency, with one standard deviation from the mean, of Ni at pH 5 (○), pH 6 (◇), pH 7 (△), and pH 8 (×). The initial Ni concentration is (A) 200 mg/L, (B) 1000 mg/L, and (C) 10000 mg/L.

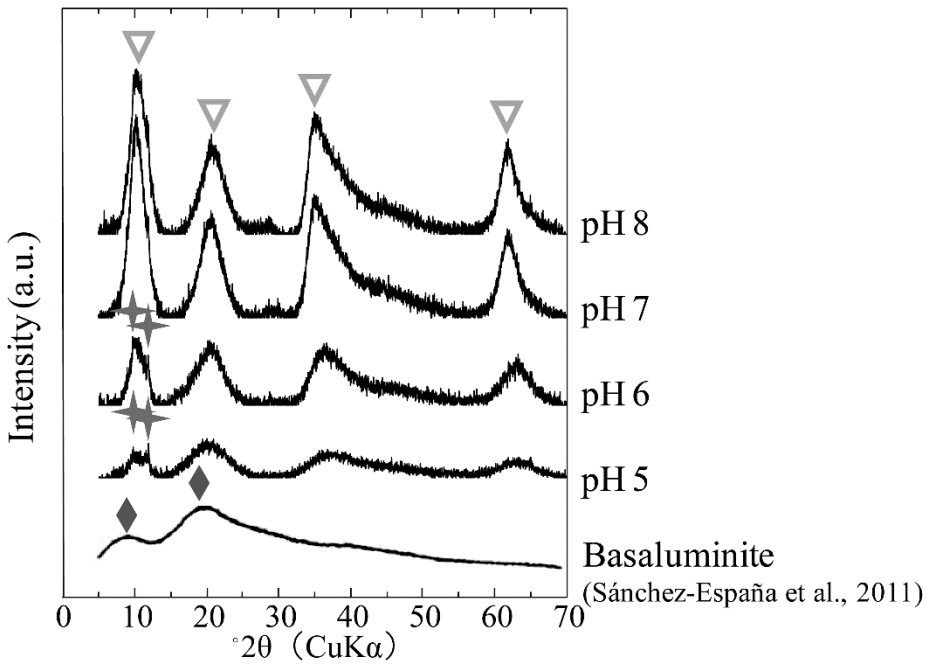

Fig. 2. X-ray diffraction patterns of precipitates (Ni = 200 mg/L, Al/Ni = 0.435) after co-precipitation. Crystalline phases: (▽) Ni-Al-LDH, (◇) basaluminite, and (＋) aluminite.

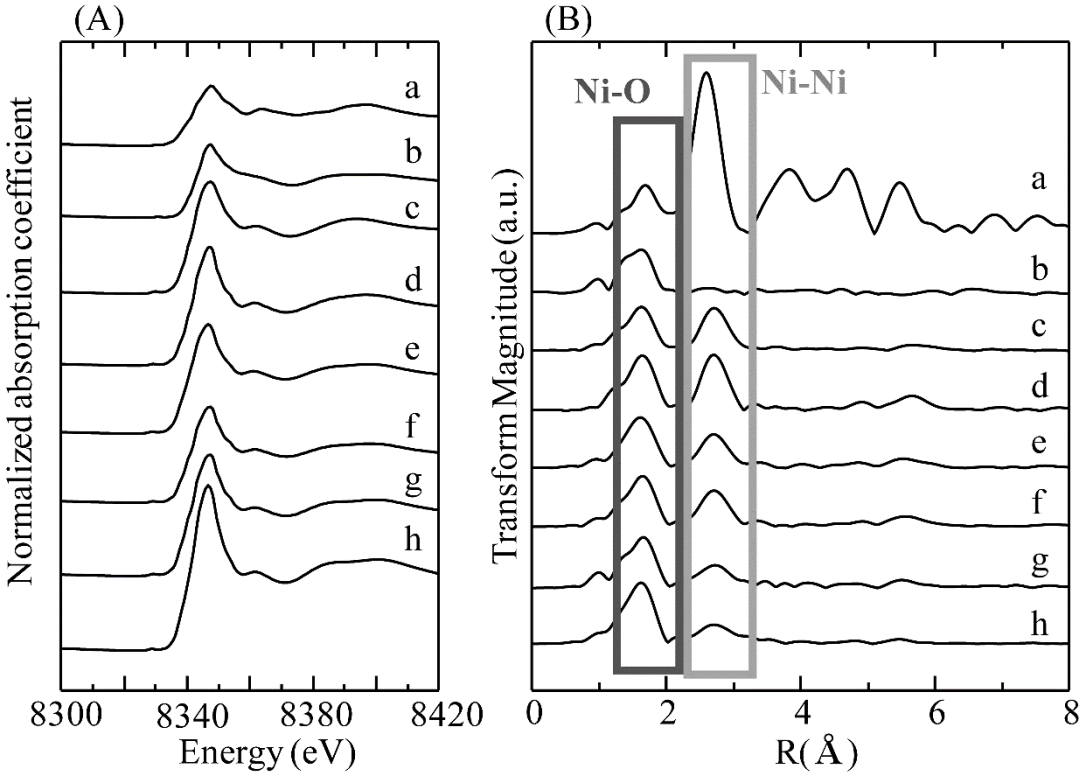

Fig. 3. (A) XANE spectrum of standards and the co-precipitated precipitates. (B) Radial distribution function profiles around Ni of standard samples: (a) NiO, (b) $NiSO4•6H_2O$, (c) Ni(OH)2, (d) takovite, and of synthesized samples with initial Ni concentrations of 1000 mg/L; and with Al/Ni ratio 0.435: (e) pH 8, (f) pH 7, (g) pH 6, (h) pH 5.

3.2. Adsorption properties of Ni to the precipitated phases

Adsorption experiments were carried out to evaluate Ni adsorption behavior of LDH and basaluminite quantitatively. Before this experiments, single-phase LDH and basaluminite[32,33] were synthesized. The results showed that only a small amount of Ni^{2+} was adsorbed to both LDH and basaluminite though basaluminite has a higher adsorption capacity than LDH (Fig. 4 (A)). This suggests that significant amounts of Ni ions were unlikely to be adsorbed onto LDH and basaluminite. The Zeta potentials of LDH and basaluminite before and after the adsorption experiments are shown in Fig.4 (B). The Zeta potential is the electric potential in a “sliding surface” at the interface of minerals and liquid phases. Since an inner-sphere complex is formed inside the

sliding surface, a significant change occurs in the zeta potential. However, as the outer-sphere complex is distributed to the diffusion layer: then outside of the sliding surface, the zeta potential does not change. When comparing the zeta potentials before and after the Ni adsorption experiments, the differences suggest that Ni becomes adsorbed to LDH as outer-sphere complexes because there is little change in the values measured before and after the adsorption experiments. A part of the Ni was inside the sliding surface and adsorbed to basaluminite, though the adsorbed amount of Ni ions here is quite small in basaluminite.

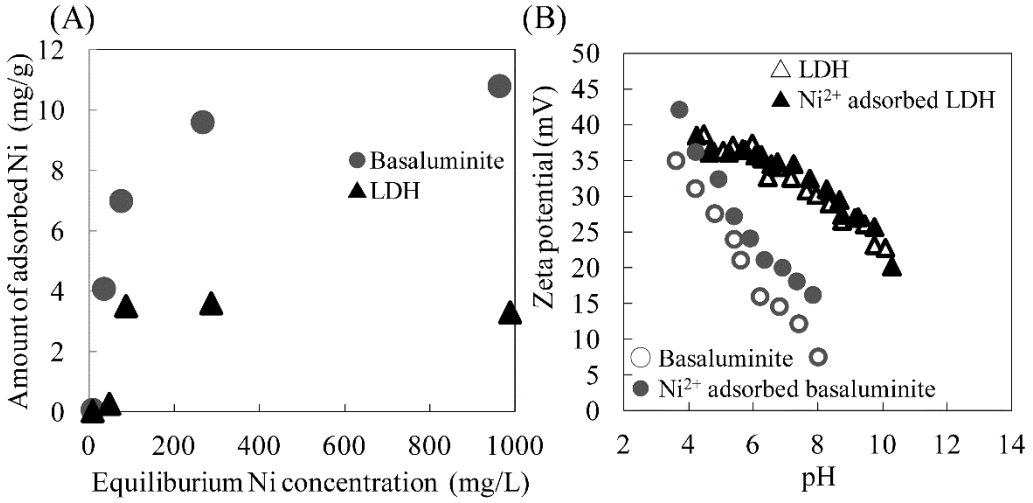

Fig. 4. (A) Adsorption isotherm of Ni for synthesized basaluminite and LDH and (B) zeta potential of the LDH and basaluminite before and after adsorption the experiments as a function of pH.

3.3. Distribution of Ni in the solid phase after co-precipitation

The percentage of the extracted and adsorbed fractions of Ni and SO_4^{2-} are shown in Fig. 5. The ratios of extracted Ni and SO_4^{2-} are not different in the experiments with different initial Ni concentrations. From the results, the extracted Ni and SO_4^{2-} decreased with increasing pH and amounts of added Al ions. The XRD patterns (not shown) showed no change in the pH 7 and 8 samples before and after the extraction experiments. This result indicates that the precipitated LDH did not dissolve. As noted above, at pH 5 and 6, a small amount of Ni ions were adsorbed on the main minerals, incorporated into LDH and taken up by the basaluminite. However, since the extracted Ni and SO_4^{2-} show similar changes, the Ni adsorbed to them and taken up by the basaluminite can be simply extracted from the sediment and at disposal sites. At pH 7 and 8, it is

suggested that Ni cannot easily be extracted until LDH dissolves because Ni was incorporated into the structure of the LDH. From the above results, if LDH is selectively precipitated, Ni will be stably incorporated into LDH.

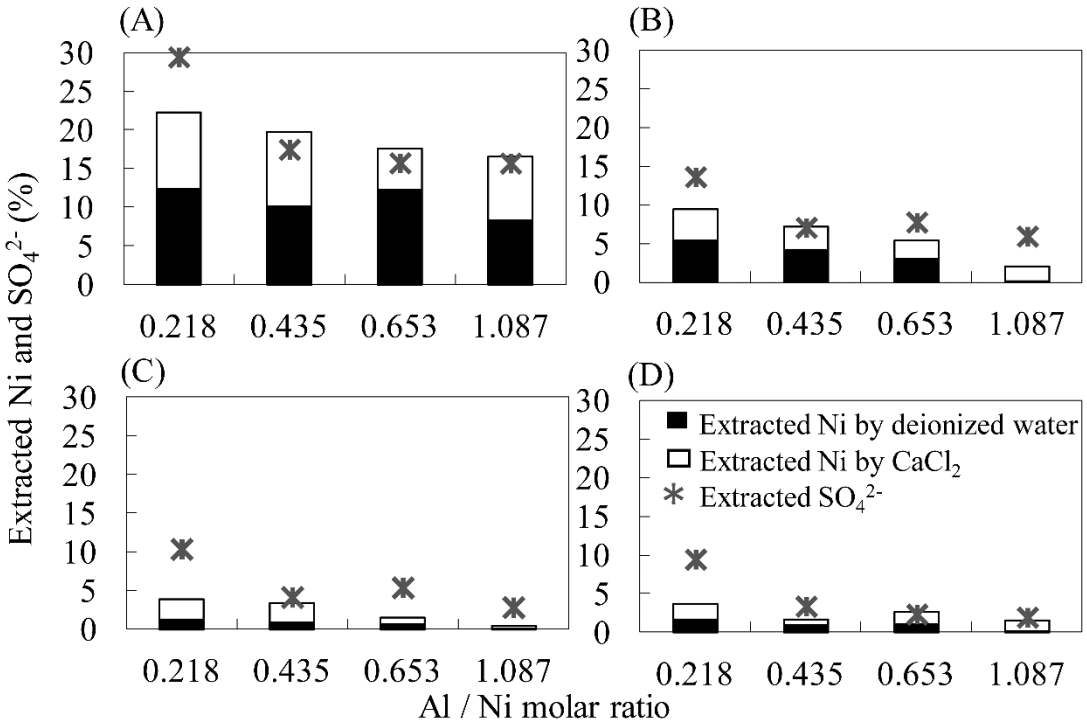

Fig. 5. Percentage of extracted and adsorbed fractions of Ni and SO_4^{2-} in the experiment with 200 mg/L Ni ion at (A) pH 5, (B) pH 6, (C) pH 7, and (D) pH 8.

3.4. Geochemical modeling of the formation of Ni-Al-LDH

3.4.1 Thermodynamic properties of Ni-Al-LDH

Geochemical modeling was carried out using ACT2 and React as in The Geochemist's Workbench version 11 to examine whether the experimental results obtained here are thermodynamically consistent with the formation of Ni-Al-LDH. Thermodynamic data for Ni-Al-LDH, basaluminite, aluminite, and sulfates and hydroxides of Al and Ni was from the thermodynamic database "Thermoddem", released by BRGM (French geological survey) [34]. The solubility product of basaluminite and aluminite were obtained from previous studies [19,30,35], and for sulfates and hydroxides of Al and Ni from the database by the Lawrence Livermore National Laboratory [36] and Visual Minteq's thermodynamic database [37], respectively. No thermodynamic data is available due to the wide variations in the chemical compositions of LDH, such as interlamellar anions, combinations of divalent and trivalent cations, and the solubility product of Ni-Al-LDH was estimated as follows.

In previous studies [29,38], the solubility products of LDHs with different anions were calculated based on their chemical compositions and thermodynamic data for their end-products such as hydroxides, sulfates, and carbonates. The thermodynamic data for these compounds were calculated from the enthalpies of formation measured by acid-solution calorimetry and solubility product constants based on solubility measurements, and the solubility products of Ni-Al-LDHs were calculated using the model in previous studies [29,38].

First, the free energies of formation ($\Delta_f G^o_{298}$) of Ni-Al-LDH ($Ni_{1-x}Al_x(OH)_2(SO_4)_{x/2} \cdot mH_2O$) were estimated by calculating values for each compound and adding these together.

$$\Delta_f G^o_{298} = \frac{x}{2}\Delta H_{NiSO_4} + x\Delta G_{Al(OH)_3} + \left(1-\frac{3}{2}x\right)\Delta G_{Ni(OH)_2} + m\Delta G_{H_2O} \quad (1)$$

The composition of LDH in the precipitated phase was not clear from the experimental results, and the X in the chemical formula for LDH that is the substituted ratio of divalent metal to trivalent metal was respectively set to 0.20, 0.25, and 0.30 in this modeling. In addition, m (the quantity of interlayer water) was set to 0.60 as about 11 wt% was interlayer water, from the thermogravimetric analysis. As a result of the calculations, the $\Delta_f G^o_{298}$ values of LDH were estimated as $\Delta_f G^o_{298}$ =-781.95 kJ/mol (x=0.2), $\Delta_f G^o_{298}$ =-827.10 kJ/mol (x=0.25), and $\Delta_f G^o_{298}$ =-899.33 kJ/mol (x=0.33).

Next, the free energies of the reaction ($\Delta_{rxn} G^o_{298}$) of Ni-Al-LDH were calculated by the following reaction,

$Ni_{1-x}Al_x(OH)_2(SO_4)_{x/2} \cdot mH_2O + 2H^+ (aq) = (1-x)Ni^{2+} (aq) + xAl^{3+} (aq) + \frac{x}{2}SO_4^{2-} (aq) + (m+2)H_2O$ (2)

and the solubility product can be simply determined using the following equation.

$\Delta_{rxn}G^{o}_{298} = -RT\ln(K_{sp}) = -2.303RT\log(K_{sp})$

where T = 298.15 K (temperature) and R = 8.314 J / mol · K (ideal gas constant).

As a result of the calculations, the solubility product constants of LDH were estimated as: $\log(K_{sp})$ = 7.64 (x=0.2), $\log(K_{sp})$ = 6.88 (x=0.25), and $\log(K_{sp})$ = 5.66 (x=0.33).

The end-product used in calculating equations (1) and (2), the enthalpy and free energy of formation at 298.15 K and 1bar were adopted from the values that are described in[39,40].

3.4.2. Thermodynamic considerations for the Ni-Al-LDH in precipitation processes

Fig. 6 shows the stability diagram for Al minerals in the Ni-Al-SO_4-H_2O system. In the diagram, the boundary of basaluminite and LDH shifted by the different Al/Ni ratios of LDH. From the XRD results after the co-precipitation, basaluminite was mainly precipitated at pH 5, basaluminite and LDH at pH 6, and LDH was mainly precipitated at pH 7 and 8. Comparing the phase diagram with the XRD patterns, modeling results of all cases were consistent with the results of the mineralogical characterization when the Al/Ni ratio of the precipitated LDH is assumed to be 0.33.

The reaction model results using React for the Ni^{2+} concentration in solution and the mineral species obtained by adding NaOH solution to Ni-containing wastewater with concentration conditions similar to the co-precipitation are shown in Fig.7 (A) and (B) respectively. In this reaction model, the Al/Ni ratio of precipitated LDH was set to 0.33. In the Al ion addition method, the small amount of Ni removed from solution and LDH precipitated despite being plotted to be in a stable zone of basaluminite at pH 5 (shown in Fig. 6) suggests that the Ni ions rather than Ni ions are taken up in the basaluminite or aluminite, as described 3.1.2. In addition, the Ni concentrations in the experiments were higher than those of the modeling at pH 6 because the LDH began to be precipitated around pH 6 and the solutions after the co-precipitation experiments were collected before much of Ni was precipitated as LDH. The Ni concentrations at pH 7 and 8 with the Al ion addition method and at pH 5–8 in the conventional method plotted along the curves of the modeling results. As mentioned in Section 3.1.1, the removed percentage of Ni was rising steadily with increasing the initial Ni concentration. This is because LDH starts to be precipitated from a low pH (around pH 5.4) and the amount of Ni incorporated into the LDH increased. (data not shown).

In addition, the mineral species appearing in the model were consistent with those in the XRD patterns. This shows that the reaction modeling results were a good reflection of the experimental results for the removal efficiency and kinds of mineral species.

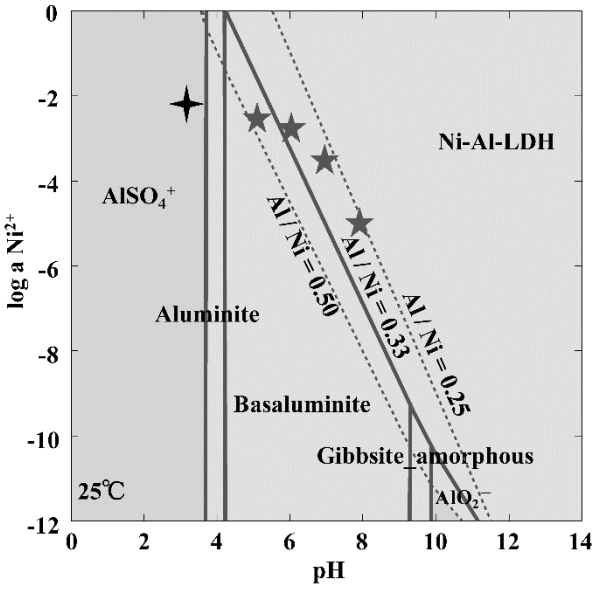

Fig. 6. Stability diagram of Al minerals in the Ni-Al-SO_4-H_2O system (Ni 200 mg/L, Al/Ni=0.435). Initial solution (＋) and solution at 5–8 after co-precipitation(★).

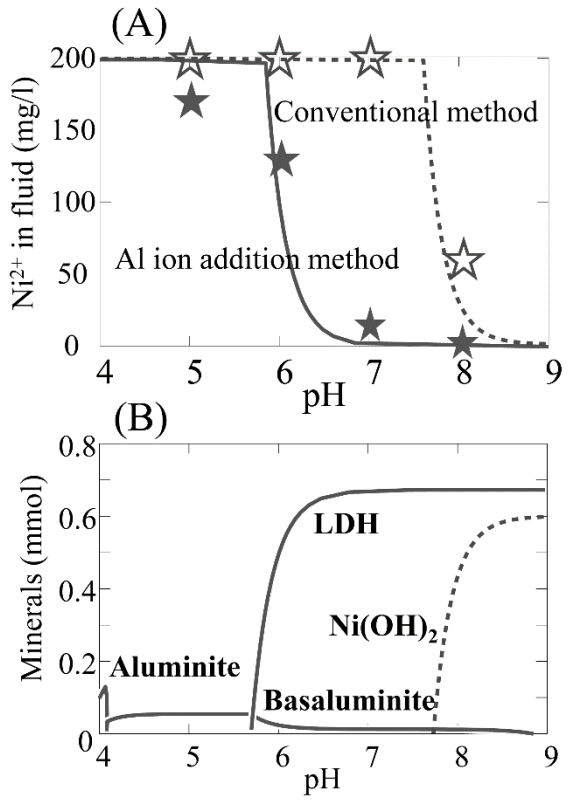

Fig. 7. Reaction models for Ni^{2+} in fluid (A) and minerals (B) in the conventional method and the Al ion addition method. Ni^{2+} 200 mg/L, Al^{3+} 40 mg/L, and SO_4^{2-} 5.6 mmol/L (——); Ni^{2+} 200 mg/L,

Al^{3+} 0 mg/L, and SO_4^{2-} 3.4 mmol/L (･･･) in the initial solutions. Ni concentrations at pH 5-8 after co-precipitation experiments in the conventional method (☆) and in the Al ion addition method (★).

Stability diagrams with the conventional method and the Al ion addition method are shown in Fig. 8. These diagrams show that the stability field of Ni-LDH is wider than that of the $Ni(OH)_2$, and that Al ion addition promotes the precipitation of LDH, which removes Ni at pH values lower than the conventional method that precipitated $Ni(OH)_2$. Therefore, Ni removal from wastewater is possible at lower pH values when LDH is used as the precipitating phase. In addition, pH of rainwater is neutral at disposal sites, so $Ni(OH)_2$ as precipitates would be dissolved and leached in excess of Ni environmental standard, whereas since LDH exists stably without dissolving in neutral pH, Ni would not exceed the value.

From the above, the $Ni(OH)_2$ precipitated in the conventional method may dissolve at the disposal site and two-step pH adjustment is required in the wastewater treatment (Fig. 9 (A)), whereas in the Al ion addition method it is possible to selectively precipitate the stable LDH present at disposal sites with a one-step pH adjustment (Fig. 9 (B)).

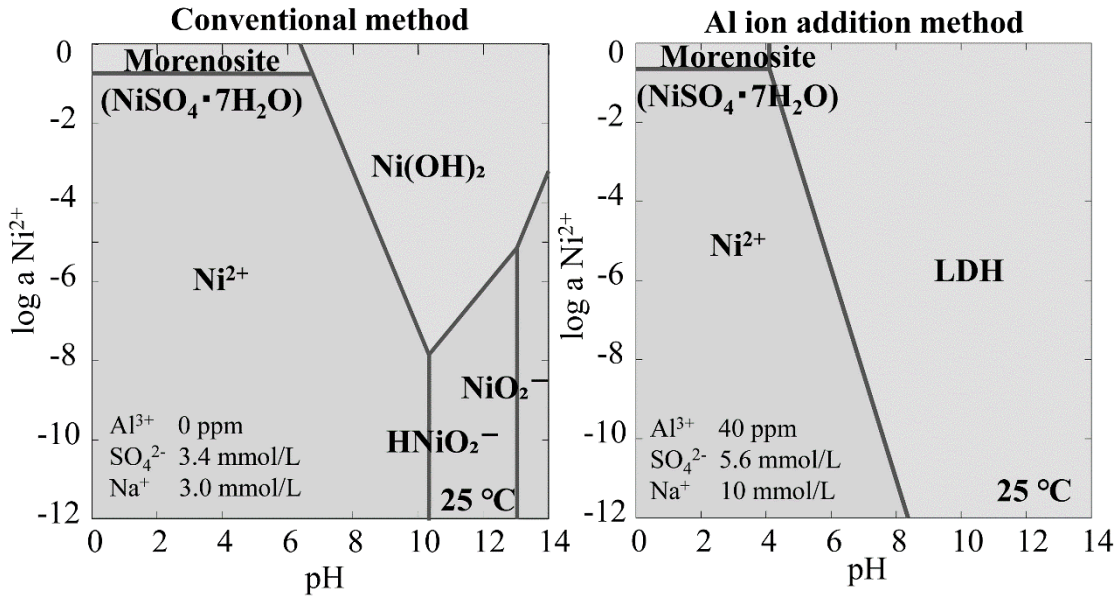

Fig. 8. Stability diagrams of (left panel) the conventional method (Ni-SO_4-H_2O system) and (right panel) the Al ion addition method (Ni-Al-SO_4-H_2O system).

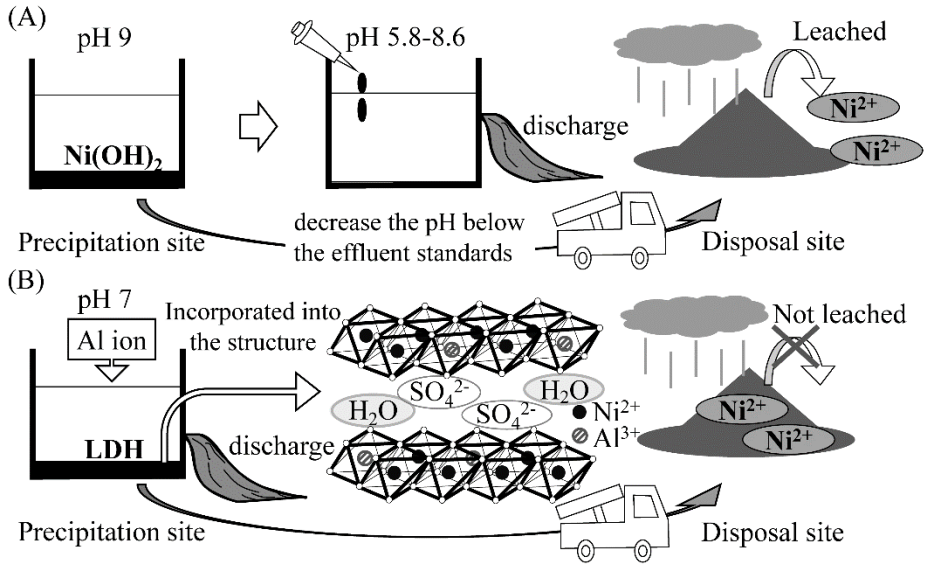

Fig. 9. Behavior of Ni^{2+} at the precipitation and disposal sites in (A) conventional method and (B) Al ion addition method.

3.4.3. Geochemical modeling applied to the Al ion addition method in various conditions

The geochemical modeling results are in good agreement with the experimental results of this study. However, it is necessary to examine whether this model applies to and can be used for wastewater treatment with various Ni concentrations in order to apply the Al ion addition method. To establish this the following section attempts to calculate the amount of added Al ions and treatment pH by using available data with Ni-containing wastewaters with various Ni concentrations and a given SO_4^{2-} concentration (1000 mg/L), adjusted to pH 5.0–8.0 (by adding NaOH solution) and applying the Al ion addition method. The reaction model results for the Ni^{2+} concentration in the solution and the mineral species plotted the results are shown in Fig. 10. In the conventional method, Ni is precipitated as hydroxides and the Ni concentration became 1 mg/L at pH 9.1. In the Al addition method, it is possible to remove Ni which is precipitated as LDH at neutral conditions (pH 7) and at lower pH than in the conventional method, by adding a small amount of Al ions (2, 16, 160 mg/L with wastewater where the Ni concentration is 10, 100, 1000 mg/L, respectively). From the above results and using this model, it is possible to calculate the amount of Al ions and additive agents necessary for use in actual wastewater treatment operations and to estimate the removal efficiency and mineral species.

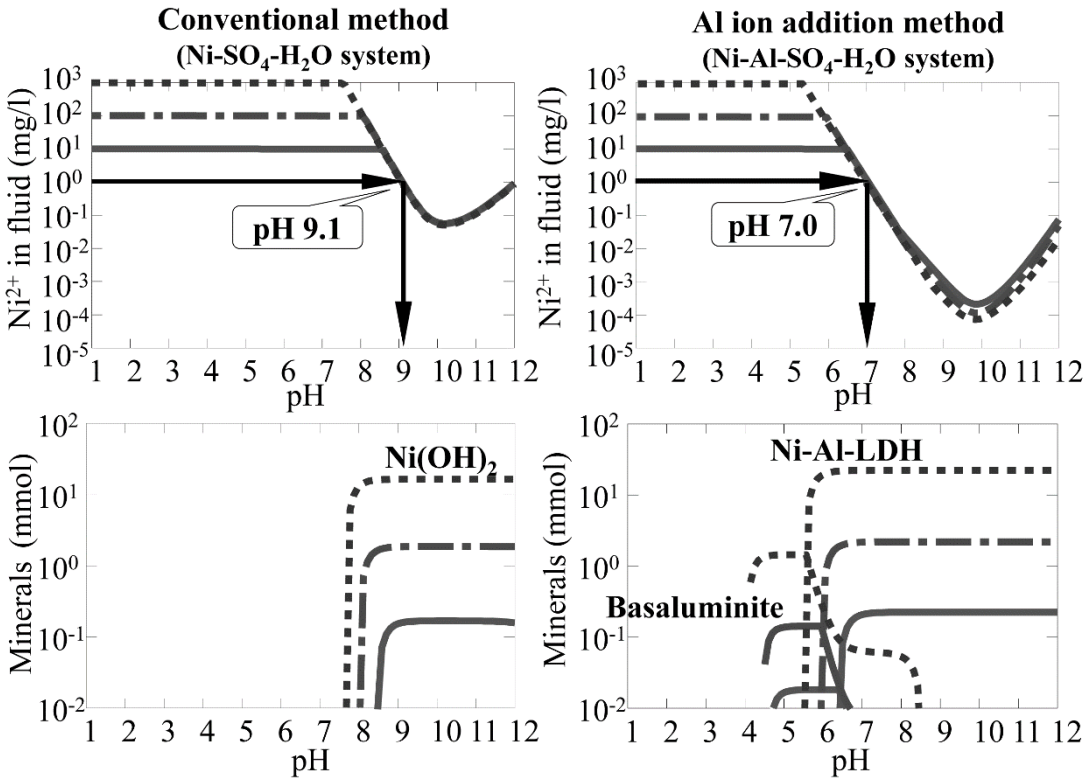

Fig. 10. Reaction models for Ni^{2+} in the fluid and minerals in (left) the conventional method and (right) the Al ion addition method with (SO_4^{2-} 1000 mg/L) at 25℃. The broken arrows in the top row shows where the target Ni concentrations are achieved. Left panels (conventional method): Ni^{2+} 10 mg/L (—), Ni^{2+} 100 mg/L (－・－), and Ni^{2+} 1000 mg/L (・・・) of the initial solutions. Right panels (Al ion addition method): Ni^{2+} 10 mg/L and Al^{3+} 2 mg/L (—), Ni^{2+} 100 mg/L and Al^{3+} 16 mg/L (－・－), and Ni^{2+} 1000 mg/L and Al^{3+} 160 mg/L (・・・) of the initial solutions

4. Conclusions and implications

In Ni-containing wastewater treatment, if Ni-LDH is selectively precipitated by applying the Al ion addition method developed here, the treatment (removal of Ni) will be successful under near-neutral conditions, at lower pH values than conventional methods to precipitate Ni. This method makes it possible to reduce the acid and alkaline neutralization agent additions. In addition, since Ni becomes incorporated into the structure of LDH especially at pH 7 and 8, it would be possible to stabilize the waste product at a wider range of pH than in conventional methods.

A thermodynamic geochemical model was able to reproduce experimental results in terms of precipitated phases as well as of the Ni removal efficiency, and would allow optimizing the Al

addition to wastewater in actual water treatment. The model confirms that it is possible to reduce Ni concentrations to below the legally mandated effluent standard when Ni-LDHs are precipitated by adding a small amount of Al ions.

In the Al ion addition method, aluminum sulfate, a by-product of the paper industry, is available as a dissolved Al source that is readily available. Employing the method developed here would lead to a reduction in neutralization agent volumes and process steps because the coagulation-sedimentation process can be carried out at neutral conditions. From the above reasons, it will be possible to optimize the neutralization process and the cost of the materials needed in the addition to the wastewater may be reduced in actual wastewater treatment.

Conflicts of interest and funding

The authors wish to declare that there are no conflicts of interest in this study and no special funding was provided (materials and equipment were what is commonly available in the laboratory).

Acknowledgements

This work was conducted under the approval of the Photon Factory Program Advisory Committee at the BL-7C (Proposal No. 2010G583) of the Photon Factory in the High Energy Accelerator Research Organization, Tsukuba City, Ibaraki Prefecture, Japan. The authors wish to thank the anonymous reviewers for their useful comments.

References

[1] International Nickel Study Group, World Nickel Statistics. (2015). http://www.insg.org/prodnickel.aspx (accessed July 25, 2016).

[2] AME Group, Nickel Feature Article–Nickel Mine Grade Decline. (n.d.). http://www.amegroup.com/Website/FeatureArticleDetail.aspx?faId=159 (accessed July 25, 2016).

[3] B. Cai, L. Xie, D. Yang, J.-P. Arcangeli, Toxicity evaluation and prediction of toxic chemicals on activated sludge system., Journal of Hazardous Materials. 177 (2010) 414–419. doi:10.1016/j.jhazmat.2009.11.152.

[4] E. El Bestawy, S. Helmy, H. Hussein, M. Fahmy, Optimization and/or acclimatization of activated sludge process under heavy metals stress, World Journal of Microbiology and

Biotechnology. 29 (2013) 693–705. doi:10.1007/s11274-012-1225-9.

[5] S.A. Ong, E. Toorisaka, M. Hirata, T. Hano, Adsorption and toxicity of heavy metals on activated sludge, ScienceAsia. 36 (2010) 204–209. doi:10.2306/scienceasia1513-1874.2010.36.204.

[6] C.K. Hope, T.R. Bott, Laboratory modelling of manganese biofiltration using biofilms of Leptothrix discophora, Water Research. 38 (2004) 1853–1861. doi:10.1016/j.watres.2003.12.031.

[7] N.K. Srivastava, C.B. Majumder, Novel biofiltration methods for the treatment of heavy metals from industrial wastewater, Journal of Hazardous Materials. 151 (2008) 1–8. doi:10.1016/j.jhazmat.2007.09.101.

[8] A. Jang, S.M. Kim, S.Y. Kim, S.G. Lee, I.S. Kim, Effects of heavy metals (Cu, Pb, and Ni) on the compositions of EPS in biofilms, Water Science and Technology. 43 (2001) 41–48.

[9] A. Özverdi, M. Erdem, Cu2+, Cd2+ and Pb2+ adsorption from aqueous solutions by pyrite and synthetic iron sulphide, Journal of Hazardous Materials. 137 (2006) 626–632. doi:10.1016/j.jhazmat.2006.02.051.

[10] M. Iqbal, A. Saeed, S.I. Zafar, FTIR spectrophotometry, kinetics and adsorption isotherms modeling, ion exchange, and EDX analysis for understanding the mechanism of Cd2+ and Pb2+ removal by mango peel waste, Journal of Hazardous Materials. 164 (2009) 161–171. doi:10.1016/j.jhazmat.2008.07.141.

[11] B. Alyüz, S. Veli, Kinetics and equilibrium studies for the removal of nickel and zinc from aqueous solutions by ion exchange resins, Journal of Hazardous Materials. 167 (2009) 482–488. doi:10.1016/j.jhazmat.2009.01.006.

[12] M.Q. Jiang, X.Y. Jin, X.Q. Lu, Z.L. Chen, Adsorption of Pb(II), Cd(II), Ni(II) and Cu(II) onto natural kaolinite clay, Desalination. 252 (2010) 33–39. doi:10.1016/j.desal.2009.11.005.

[13] M. Mohsen-Nia, P. Montazeri, H. Modarress, Removal of Cu2+ and Ni2+ from wastewater with a chelating agent and reverse osmosis processes, Desalination. 217 (2007) 276–281. doi:10.1016/j.desal.2006.01.043.

[14] H. Bessbousse, T. Rhlalou, J.F. Verchère, L. Lebrun, Sorption and filtration of Hg(II) ions from aqueous solutions with a membrane containing poly(ethyleneimine) as a complexing polymer, Journal of Membrane Science. 325 (2008) 997–1006. doi:10.1016/j.memsci.2008.09.035.

[15] I. Kabdaşli, T. Arslan, T. Ölmez-Hanci, I. Arslan-Alaton, O. Tünay, Complexing agent and heavy metal removals from metal plating effluent by electrocoagulation with stainless steel electrodes, Journal of Hazardous Materials. 165 (2009) 838–845. doi:10.1016/j.jhazmat.2008.10.065.

[16] F.M. Pang, S.P. Teng, T.T. Teng, A.K. Mohd Omar, Heavy metals removal by hydroxide precipitation and coagulation-flocculation methods from aqueous solutions, Water Quality

Research Journal of Canada. 44 (2009) 174–182.

[17] K.A. Baltpurvins, R.C. Burns, G.A. Lawrance, A.D. Stuart, Use of the solubility domain approach for the modeling of the hydroxide precipitation of heavy metals from wastewater, Environmental Science and Technology. 30 (1996) 1493–1499. doi:10.1021/es950421u.

[18] S.B. Rao Y. Surampalli, Say Kee Ong, Eric Seagren, Julio Nuno, Natural Attenuation Of Hazardous Wastes, 2004.

[19] S. Tumiati, G. Godard, N. Masciocchi, S. Martin, D. Monticelli, Environmental factors controlling the precipitation of Cu-bearing hydrotalcite-like compounds from mine waters. The case of the “Eve verda” spring (Aosta Valley, Italy), European Journal of Mineralogy. 20 (2008) 73–94. doi:10.1127/0935-1221/2008/0020-1782.

[20] H. Okamoto, K. Morimoto, S. Anraku, T. Sato, T. Yoneda, A novel remediation method learnt from natural attenuation process for Cu- and Zn-bearing wastewater, Clay Science. 14 (2010) 203–210.

[21] S. Miyata, Physico-Chemical Properties of Synthetic Hydrotalcites in Relation to Composition, Clays and Clay Minerals. 28 (1980) 50–56. doi:10.1346/CCMN.1980.0280107.

[22] F. Cavani, F. Trifi r, A. Vaccari, Hydrotalcite-type anionic clays: preparation, properties and applications, Catalysis Today. 11 (1991) 173–301.

[23] T.M. Adams, J.R. Sanders, The effects of pH on the release to solution of zinc, copper and nickel from metal-loaded sewage sludges, Environmental Pollution. Series B, Chemical and Physical. 8 (1984) 85–99. doi:10.1016/0143-148X(84)90020-X.

[24] J.R. Sanders, M.I. El Kherbawy, The effect of pH on zinc adsorption equilibria and exchangeable zinc pools in soils, Environmental Pollution. 44 (1987) 165–176. doi:10.1016/0269-7491(87)90001-7.

[25] M.K. Titulaer, J.B.H. Jansen, J.W. Geus, The quantity of reduced nickel in synthetic takovite: Effects of preparation conditions and calcination temperature, Clays and Clay Minerals. 42 (1994) 249–258. doi:10.1346/CCMN.1994.0420303.

[26] S. Abelló, D. Verboekend, B. Bridier, J. Pérez-Ramírez, Activated takovite catalysts for partial hydrogenation of ethyne, propyne, and propadiene, Journal of Catalysis. 259 (2008) 85–95. doi:10.1016/j.jcat.2008.07.012.

[27] T. Kameda, H. Takeuchi, T. Yoshioka, NiAl layered double hydroxides modified with citrate, malate, and tartrate: Preparation by coprecipitation and uptake of Cu2 from aqueous solution, Journal of Physics and Chemistry of Solids. 72 (2011) 846–851. doi:10.1016/j.jpcs.2011.03.003.

[28] M.E. Rivas, J.L.G. Fierro, R. Guil-López, M. a. Peña, V. La Parola, M.R. Goldwasser,

Preparation and characterization of nickel-based mixed-oxides and their performance for catalytic methane decomposition, Catalysis Today. 133–135 (2008) 367–373. doi:10.1016/j.cattod.2007.12.045.

[29] E. Peltier, R. Allada, A. Navrotsky, D.L. Sparks, Nickel solubility and precipitation in soils: A thermodynamic study, Clays and Clay Minerals. 54 (2006) 153–164. doi:10.1346/CCMN.2006.0540202.

[30] J. Sánchez-España, I. Yusta, M. Diez-Ercilla, Schwertmannite and hydrobasaluminite: A re-evaluation of their solubility and control on the iron and aluminium concentration in acidic pit lakes, Applied Geochemistry. 26 (2011) 1752–1774. doi:10.1016/j.apgeochem.2011.06.020.

[31] F. Farges, G.E. Brown Jr., P.-E. Petit, M. Munoz, Transition elements in water-bearing silicate glasses / melts . Part I . A high-resolution and anharmonic analysis of Ni coordination environments in crystals , glasses , and melts, 65 (2001) 1665–1678.

[32] Y. Zhao, F. Xiao, Q. Jiao, Hydrothermal synthesis of Ni/Al layered double hydroxide nanorods, Journal of Nanotechnology. 2011 (2011) 4–9. doi:10.1155/2011/646409.

[33] J. Prietzel, B. Mayer, Isotopic fractionation of sulfur during formation of basaluminite, alunite, and natroalunite, Chemical Geology. 215 (2005) 525–535. doi:10.1016/j.chemgeo.2004.06.048.

[34] P. Blanc, A. Lassin, Thermoddem: a database devoted to waste minerals, BRGM, Orléans, France. Http://thermoddem.brgm.fr/. (2007). http://thermoddem.brgm.fr/Fichiers/Thermoddem_presentation.pdf.

[35] F. Adams, Z. Rawajfih, Basaluminite and Alunite: A Possible Cause of Sulfate Retention by Acid Soils, Soil Science Society of America Journal. 41 (1977) 686–692. doi:10.2136/sssaj1977.03615995004100040013x.

[36] J.M. Delany, S.R. Lundeen, The LLNL Thermochemical Database, Lawrence Livermore National Laboratory Report UCRL -21658. (1989) 150. http://scholar.google.de/scholar?q=database+llnl+thermochemical&btnG=&hl=de&as_sdt=0,5#2.

[37] J.. Gustafsson, Visual MINTEQ Version 3.0, Royal Institute of Technology. Department of Land and Water Resources Engineering, Stockholm, Sweden. (2012).

[38] R.K. Allada, A. Navrotsky, H.T. Berbeco, W.H. Casey, Thermochemistry and aqueous solubilities of hydrotalcite-like solids., Science (New York, N.Y.). 296 (2002) 721–723. doi:10.1126/science.1069797.

[39] R. a. Robie, B.S. Hemingway, J.R. Fisher, Thermodynamic properties of minerals and related substances at 298.15 K and 1 bar (10^5 Pascals) pressure and at higher temperatures, U.S. Geological Survey Bulletin. 2131 (1995). http://pubs.usgs.gov/bul/1259/report.pdf.

[40] R. kumar Allada, E. Peltier, A. Navrotsky, W.H. Casey, C.A. Johnson, H.T. Berbeco, D.L. Sparks, Calorimetric determination of the enthalpies of formation of hydrotalcite-like solids and their use in the geochemical modeling of metals in natural waters, Clays and Clay Minerals. 54 (2006) 409–417. doi:10.1346/CCMN.2006.0540401.